RSC Advances

ROYAL SOCIETY OF CHEMISTRY

www.rsc.org/advances

The effect of γ-ray irradiation on the microstructure and thermal properties of polyacrylonitrile fibers

Weizhe Zhao, Yonggen Lu*, Junqi Jiang, Leiyang Hu, Liangxiao Zhou

State Key Laboratory for Modification of Chemical Fibers and Polymer Materials, College of Materials Science and Engineering, Donghua University, Shanghai, China, 201620

Abstract

In this paper, not only the effect of γ-ray irradiation on chemical structures and thermal properties of PAN fibers, but also the corresponding reaction mechanisms were investigated. We reported a new solubility measurement adopting sulfuric acid solution as a solvent to deeply discern cyclization and crosslinking reactions of PAN fibers after γ-ray irradiation. After the irradiation, the intramolecular cyclization of PAN fibers was dominant at relatively low doses (< 200 kGy), while intermolecular crosslinking in amorphous regions at higher doses. Moreover, the irradiation had an obvious effect on crystal dimensions and crystallinity but very slight on orientation for the precursor fibers. The crosslinking and cyclization mechanisms were also analyzed using Fourier transform infrared spectroscopy and differential scanning calorimetry. The thermal behavior of PAN precursor fibers demonstrated that the manipulation range of applied stress during the following thermal stabilization could be amplified by the intermolecular crosslinking due to the pre-irradiation treatment,

* Corresponding author: Tel: +86 21 67792936. E-mail address: yglu@dhu.edu.cn (Yonggen Lu).

which would be benefit for depressing the molecular disorientation during thermal stabilization.

1. Introduction

Polyacrylonitrile (PAN) fibers are one of the most important precursors for high strength and high modulus carbon fibers [1]. Prior to converting into carbon fibers, PAN fibers need to be stabilized to prevent the fibers from melting or fusing during carbonization [2-3]. During the stabilization process, cyclization, oxidation, dehydrogenation and crosslinking reactions are involved, thereby the linear molecule chains are converted into cross-linked ladder structures [4]. When these reactions take place, the high orientation of PAN molecules in precursor fibers is always hoped to be preserved, and the oxidation degree is always expected to be uniform across the fiber diameter. However, during stabilization, thermal shrinkage of the flexible and linear molecule chains usually makes the orientated molecules tend to disorient [5-7], and oxygen diffusion resistance tends to cause a nonuniform oxidation across the fiber section. Thus, new methods should be developed to induce cyclization or crosslinking below the glass transition temperature and independent of oxidation.

Very recently, ionizing radiation, such as γ-ray [8-11], electron beam [12-14], UV [15,16] and X-ray [17], has been widely used in modification of polymeric materials by initiating reactions or inducing crosslinking [18,19]. Some investigations on irradiation of PAN fibers indicated that the insolubility of molecules was increased, the initial reaction temperature was decreased, and the free radicals were preserved [20,21]. Zhao WW et al. [22] concluded that the free radicals induced by irradiation could initiate

thermal chemical reaction. Tarakanov [8] reported that irradiated PAN samples could be oxidized much more rapidly than the unirradiated ones, implying that irradiation indeed accelerated the formation of ladder structures. However, whether and how the crosslinking takes place during irradiation are far more than clear.

Some researchers deem that the crosslinked structure in irradiated PAN fibers can be determined by the insolubility in dimethylsulfoxide (DMSO) or dimethyl formamide (DMF) [9,14,15,23]. However, to our knowledge, the crosslinking can't be distinguished from cyclization using the insolubility in these solvents. Therefore, more detailed work is needed to verify the effect of the γ-ray irradiation on the structure of PAN fibers and clarify the reaction mechanism.

In this work, we report a new solubility measurement adopting sulfuric acid solution as a solvent to deeply discern cyclization and crosslinking reactions of PAN fibers after γ-ray irradiation. Combining with the insolubility in DMSO, we definitely distinguished crosslinking from cyclization and quantified the proportion of cyclization and crosslinking in irradiated fibers. Meanwhile, the thermal behaviors of unirradiated and irradiated PAN fibers are analyzed.

2. Experimental

2.1 Materials

The as-received PAN precursor fibers (wet-spun from acrylonitrile/acrylamide copolymer, and having 3000 filaments/tow, 11.21 μm average diameter, 1.174 g/cm^3 bulk density, 740 MPa tensile strength, 8 .6 GPa Young's modulus) were supplied by Mitsubishi Co., Japan and named as UN in this work.

2.2 γ-ray irradiation

The PAN fibers were winded around an aluminum tube and then irradiated with a cobalt-60 γ-ray source in air by Shanghai JPY Ion-Tech Co., Ltd.. The different doses (50, 100, 200, 300 and 400 kGy) on the fibers were used by changing the irradiation time， and the samples were named as IR-1, IR-2, IR-3, IR-4, IR-5 respectively.

2.3 Preparation of the fully cyclized structure fibers without crosslinking

A fully cyclized structure fiber （FC-F） sample was prepared by heat treatment in a batch-type furnace under nitrogen atmosphere for avoiding oxidation according to the following program: firstly, the PAN precursors were heated up to 170 ^{o}C at 5 ^{o}C min^{-1} from room temperature in this furnace, then up to 270 ^{o}C at 3 ^{o}C min^{-1}, then were taken out immediately until the final temperature arrived.

2.4 Stabilization in air at a series of constant stresses

The stabilization under a constant initial stress in air was carried out as the following procedure. Six rows of fiber tow with length of twenty centimeter, were hung under an iron rack. Initial stresses from 1.5 to 27 MPa were applied on the fiber tows respectively, by loading different weights at the fiber tow ends. The heating procedure was followed as Section 2.3 .

2.5 Characterization

The solubility of the as-received, the irradiated and the FC-F fibers were measured with sulfur acid and DMSO respectively. For the measurement of insoluble fraction in sulfur acid, the fibers were immersed into 75 wt% sulfur acid at room temperature for 24 h. The resultant insolubles were separated from the solvent by filtration, washed

several times by water, then dried in vacuum at 80 ^{o}C for 48 h and weighed to obtain the mass fraction relative to the original mass. The sulfur acid insolubles were labeled as SIR-3i, SIR-4i, SIR-5i for the fibers irradiated at 200, 300 and 400 kGy.

The insoluble fraction of the fibers in DMSO was measured by immersing the fibers into DSMO at room temperature for 24 h, then separating, weighing and calculating similarly.

Differential scanning calorimetry (DSC) measurements were performed on a TA-Q20 (TA instruments) differential scanning calorimeter at 10 ^{o}C min^{-1} under nitrogen atmosphere. The degree of cyclization (D_c) of the fibers was calculated by the exothermal enthalpy as follows [24,25].

$$D_c\% = \frac{H_0 - H_i}{H_0} \times 100 \quad (1)$$

where H_0 is the heat release of the as-received PAN fiber, H_i is the heat release of irradiated fibers at various doses.

Fourier transform infrared spectroscopy (FTIR) of KBr disks were measured on a Thermo Nicolet 8700 FTIR spectrophotometer at room temperature; 32 scans were collected at a resolution of 1 cm^{-1}.

Wide-angle X-ray diffraction (WXRD) was used to investigate the crystallite structures on a D/Max-2550 PC XRD apparatus (Cu Ka, 0.154056 nm, 40 kV, 250 mA) by arranging a fiber bundle perpendicular to the incident ray. The crystallinity (X_c) was calculated from the areas of the crystalline diffraction peaks using Bell and Dumbleton method by Origin 8.0 software shown in the literature [26].

The crystallite stack height L_c (100) and the crystallite width L_a (100) were

determined by (100) reflection, and the values were calculated using the Scherrer equation, respectively. The shape factor, *k*, was taken as 0.9 for the crystallite heights and 1.84 for the crystallite widths. The full width at half maximum (FWHM) of the diffraction peak from the azimuthal scan was used to estimate the degree of orientation (R) [27,28]

$$L = \frac{k\lambda}{\beta \cos\theta} \quad (2)$$

$$R = \frac{360 - Z_1 - Z_2}{360} \quad (3)$$

where β is the FWHM of the diffraction peak around $2\theta = 17^o$ and Z_1, Z_2 is the FWHM of the two diffraction peaks from azimuthal scan, θ is Bragg angle.

The stress and strain behaviors of the fibers were measured with a fiber bundle containing 100 filaments on a TA-Q800 (TA instruments) dynamic mechanical analysis (DMA) at 5 ^{o}C min^{-1} under a nitrogen gas flow. For stress measurements, a controlled strain of 0.05% was applied to maintain a constant length. And for strain tests, a constant force of 0.15 N (0.15 cN at each signal filament, equal to a constant stress of 12.75 MPa calculated based on the diameter of precursor fibers) was carried out on the fiber bundle.

3. Results and discussion

3.1 The effect of γ -ray irradiation on physical properties of the PAN fibers

The common thermal stabilization in air makes precursors insoluble and infusible because of the formation of cyclized and crosslinked structure in PAN molecules [2]. In order to distinguish the different reactions of cyclization and crosslinking, the solubility of the γ-ray irradiated fibers should also be concerned.

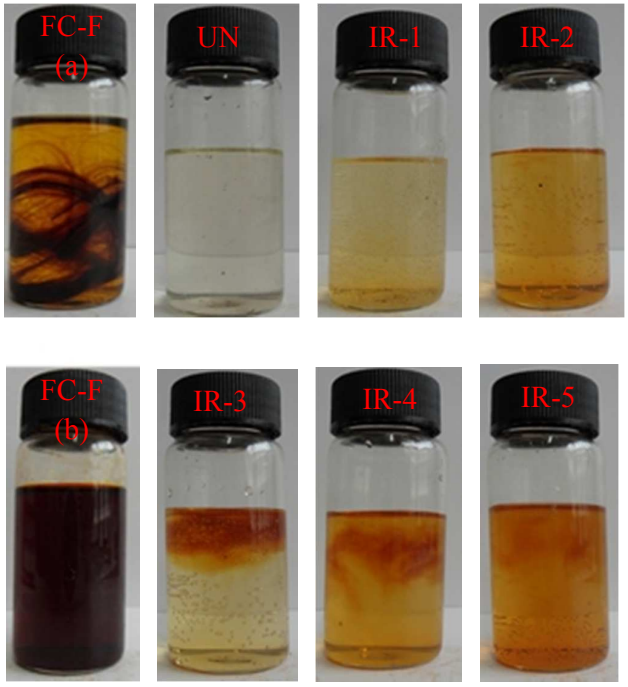

Fig. 1 - Solubility of FC-F immersed into (a) DMSO solvent and in (b) sulfur acid, and PAN fibers of UN, IR-1, IR-2, IR-3, IR-4, IR-5 in sulfur acid.

Fig.1 shows the solubilities of fully cyclized structure fibers without crosslinking (FC-F) in DMSO and sulfur acid respectively, and the solubilities of PAN fibers at various doses of 0, 50, 100, 200, 300, 400 kGy in sulfur acid. As shown in Fig.1, the FC-F isn't dissolved in DMSO even the color has a little change, however, it is fully dissolved in sulfur acid which results in the formation of reddish-brown solution. For PAN fibers, the solubility in sulfur acid decreases and the color is thicker and thicker with the increase of irradiation doses. Therefore, the results indicate the FC-F can't be dissolved in DMSO, whereas, it can be fully dissolved in sulfur acid. In other words, the DMSO solvent is unable to dissolve the cyclized structures in PAN fibers. Therefore it is for sure that the insolubility in DMSO is inadequate to verify crosslinking taking place during irradiation. However, the irradiated fibers from IR-1

and IR-2 can be but IR-3, IR-4 and IR-5 can't be completely dissolved in the sulfur acid even the solutions' color is much lighter than that from FC-F (b). Thus, it is estimated that the DMSO insoluble is related to the parts of both cyclized and crosslinked, while the sulfur acid insoluble is only related to the crosslinked part. Fig.2 (a) shows the insoluble fraction quantities of the irradiated fibers with different doses in DMSO and sulfur acid, respectively. It is noted that the insoluble fraction in DMSO increases from 13.04% at 50 kGy to 68.3% at 400 kGy monotonously. In sulfur acid, the unirradiated and the irradiated fibers at the doses of 50 and 100 kGy are dissolved completely, however, the insoluble fraction yields to approximately 31.8% at 200 kGy, and then increases gradually to 59.7% with the irradiation dose increasing to 400 kGy. What's more, the density of the fibers increases from 1.174 g/cm^3 of unirradiated fibers to 1.197 g/cm^3 of the 400 kGy irradiated fibers as shown in Fig.3, which should be resulted from the reactions induced by irradiation forming the denser structure [9]. Therefore, the phenomenon that the solutions looking more uniform from IR-3 to IR-5 can be ascribed to the fiber density increasing which made the insoluble sink and look dispersed well.

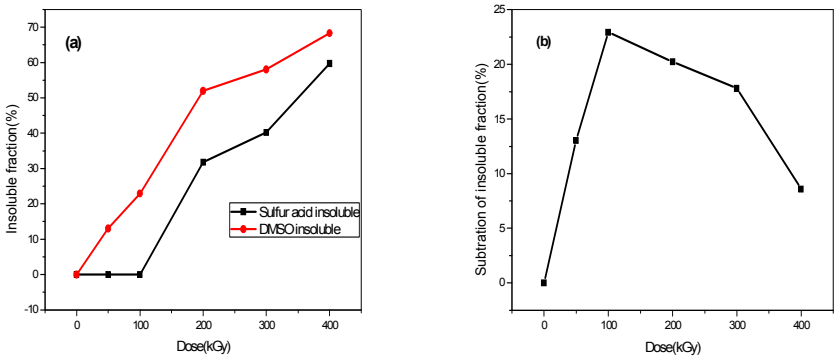

Fig. 2 - (a) DMSO and sulfur acid insoluble of the PAN fibers induced by γ-ray irradiation at various doses, respectively; (b) Subtraction of sulfur acid insoluble from DMSO insoluble.

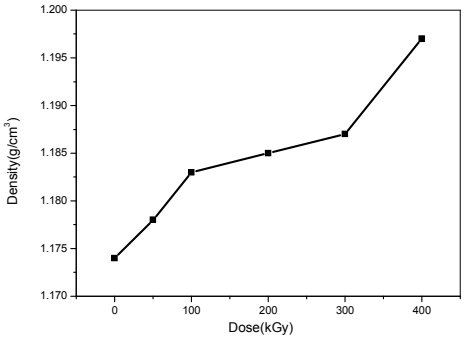

Fig. 3- The densities of the PAN fibers as a function of irradiation dose.

By subtracting the insoluble fraction curves in sulfur acid from those in DMSO, the fraction quantity of cyclization without crosslinking (we name as independent cyclization) is obtained. As shown in Fig. 2 (b), the fraction quantity of independent cyclization increases with irradiation doses increasing and reaches a maximum at 100 kGy, then decreases with further irradiation. Therefore, it is clearly found that cyclization of nitrile groups is dominant at 100 kGy and below, and further irradiation generates inter-crosslinking.

3.2 The chemical structure of the irradiated PAN fibers and the proposed mechanism of crosslinking and cyclization

In order to provide a further evidence to demonstrate the changes of chemical structure, FTIR spectra are obtained from the PAN fibers, as shown in Fig. 4. The spectrum of untreated PAN fibers shows peaks at 2245, 1627, 2940, 1678, and 1260 cm^{-1}, which correspond to the stretching vibrations of the -C≡N, -C=N- conjugated with -C=C-, $–CH_2$, -C=O in acridone rings and C-O-C respectively, and the peak at 1450 cm^{-1} is correspond to the bending vibrations of $–CH_2$. Clearly, the intensity of the bands at 2245 cm^{-1} decreases gradually with the increasing irradiation doses, and the intensity of other interesting bands at 1627 cm^{-1} increases with further irradiation. It indicates that cyclization reaction is caused by the irradiation. In addition, the absorption bands at 2940 and 1450 cm^{-1} concurrently decreases, demonstrating dehydrogenation occurs during the irradiation. The intensity of the peak at 1678 cm^{-1} increases, which means oxidation also takes place during the irradiation. Moreover, the absorption near 1260 cm^{-1} for various C-O-C stretches can be attributed to crosslinking bonds. Therefore, it is considered that cyclization, dehydrogenation and oxidation or crosslinking reactions occur during γ-ray irradiation and form a similar network structure induced by thermal stabilization. The attributions of the peaks assigned to the functional groups can be found in lots of literatures [29-33].

It is fairly agreed that how cyclization, dehydrogenation and oxidation or even crosslinking reactions take place by thermal treatment. However, how crosslinking occurs during irradiation is still not so clear. Herewith three proposed types of

crosslinking mechanism are presented in Fig. 5. Above all, backbone radicals are generated by break of C-H bond under γ-ray irradiation [21]. The first mechanism, by which so-called crosslinking of "H" type may generate by recombination of two backbone radicals or by one backbone radical adding to a nitrile group on an adjacent chain and initating cyclization, is mentioned in some literatures [9,34]. By the second mechanism, the radical transfers to the end of the chain forming terminal radical, and recombines or adds in a similar way. When the terminal radical recombines with a backbone radical or adds to a nitrile group on an adjacent chain, the crosslinking of "Y" type is formed. What needs to emphasize is the third mechanism proposed by us, by which the crosslinking takes place due to presence of oxygen. Addition of O_2 to the backbone radicals leads to the generation of backbone-peroxy radicals. Then one O atom is lost by attacking of H_2 to produce backbone-oxygen radicals [35]. After that, the backbone-oxygen radicals may recombine with C atoms on adjacent molecule chains to crosslink or add to a nitrile group on adjacent chains to initiate cyclization. Subsequently, an intermolecular oxygen crosslinking model at high irradiation doses is formed as shown in Fig. 6.

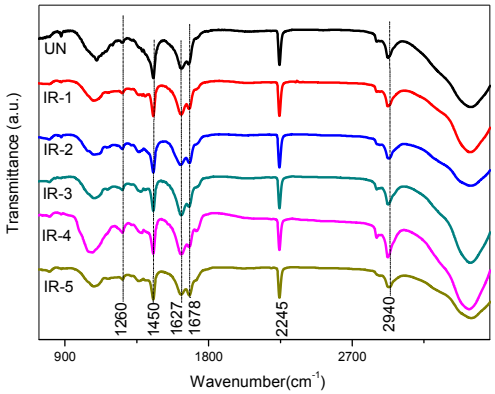

Fig. 4 - FTIR curves of PAN fibers at various doses. (a) 0 kGy; (b) 50 kGy; (c) 100 kGy; (d) 200 kGy; (e) 300 kGy; (f) 400 kGy.

Mechanism 1：

Pathway 1:

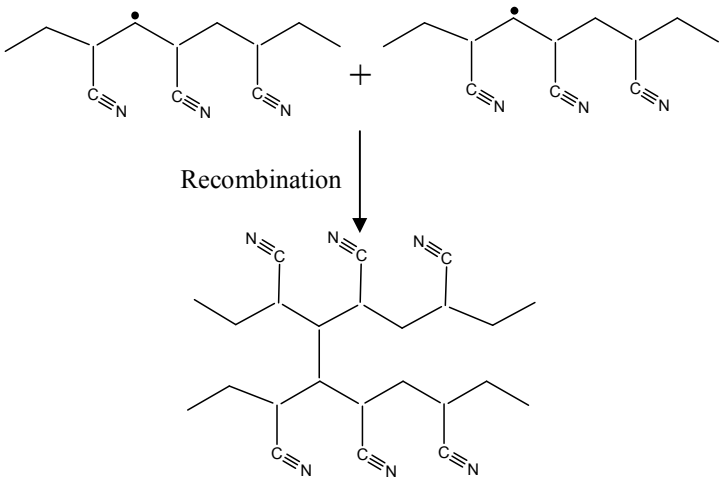

Pathway 2:

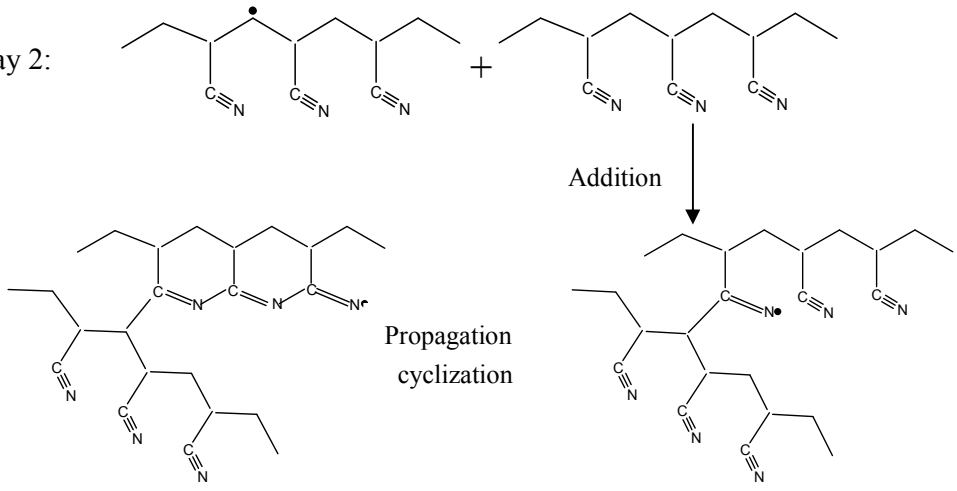

Mechanism 2：

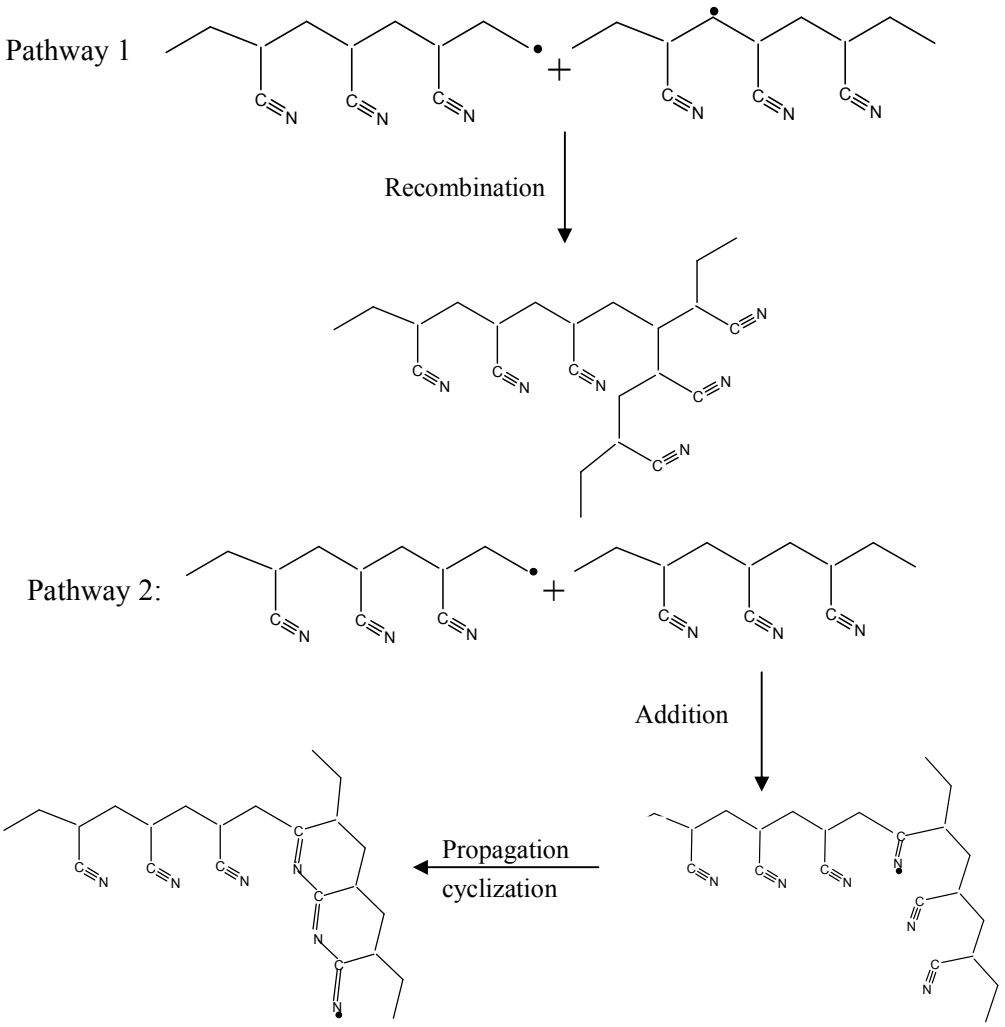

Mechanism 3：

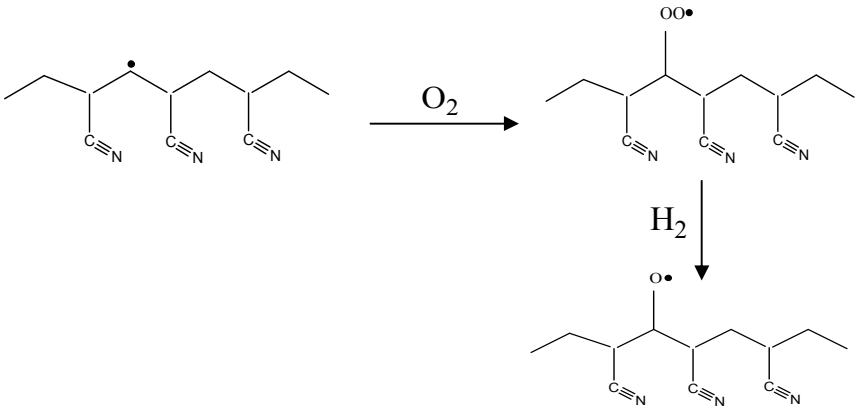

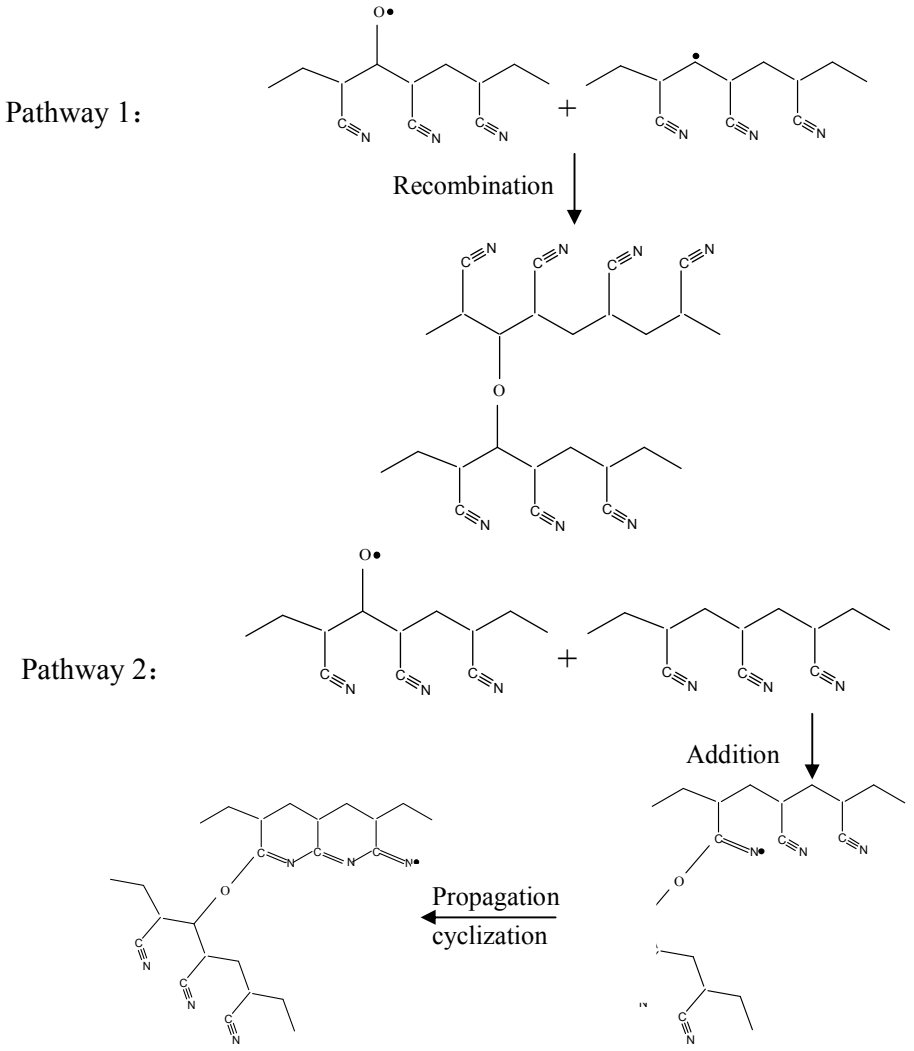

Fig. 5 - Proposed mechanism of crosslinking of PAN fibers induced by γ-ray irradiation

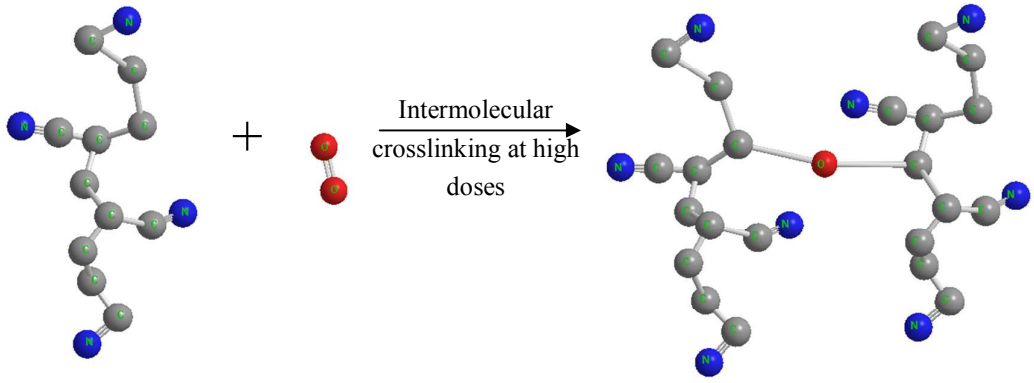

Fig. 6 - The intermolecular chain model on oxygen crosslinking at high irradiation doses

The insolubility and FTIR analysis verify the reactions of cyclization and crosslinking takes place during γ-ray irradiation, and the cyclization ratio is also determined by DSC analysis. Fig. 7 shows DSC curves of the unirradiated and irradiated PAN fibers in nitrogen atmosphere. It is noted that two exothermic peaks are found at approximately 259 and 272 ^{o}C for the unirradiated fibers, respectively, corresponding to the two step initiation of cyclization by the comonomers of acrylamide (AM) which is also similar to the reported data in the literature [36]. As anticipated, the initial reaction temperature shifts to lower temperature and the total area of exothermal peak decreases with increase of irradiation doses. However, it is curious that the temperature of the second exothermal peak increases with increasing irradiation doses, which will be interpreted later.

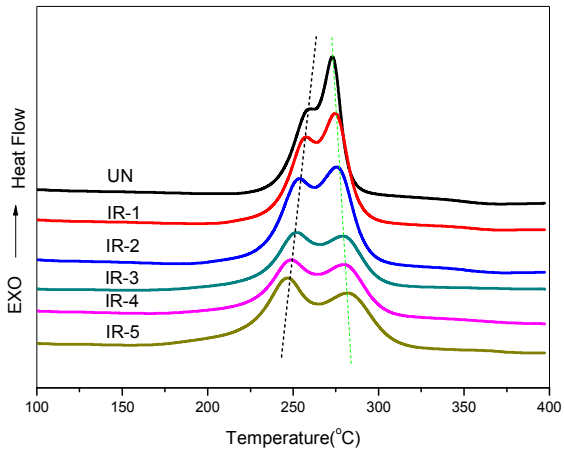

Fig. 7 - DSC curves of PAN fibers at various doses.

The D_c for each irradiated fibers is calculated by the heat release according to the formula in the experimental section and drawn in Fig. 8. It is noted that the D_c increases with increase of irradiation doses monotonically which obeys first order

reaction as we discussed elsewhere [37]. In order to quantify the relationship between D_c and irradiation doses, we assume that D_e is the maximal possible degree of cyclization in the unit volume, and the degree of newly produced cyclization (dy) in time dt of irradiation is proportional to the intensity of irradiation, I, so the equation is obtained :

$$\frac{dy}{dt} = KI(D_e - y) \quad (4)$$

where K is the scale factor.

By intergrating the Eq. (4), we get the relationship:

$$y = D_e\left[1 - \exp(-KIt)\right] = D_e\left[1 - \exp(-Kx)\right] \quad (5)$$

where $x = It$ is the irradiation dose.

Based on the experiment data of D_c after irradiation, we regressed the data according to Eq. (5) (the line in Fig. 8) by Origin 8.0 software and the results matched extremely well with the experiment data ($R^2 = 0.9785$). The parameters D_e and K were regressed as follows:

$$y = 0.1675\left[1 - \exp(-0.004x)\right] \quad (6)$$

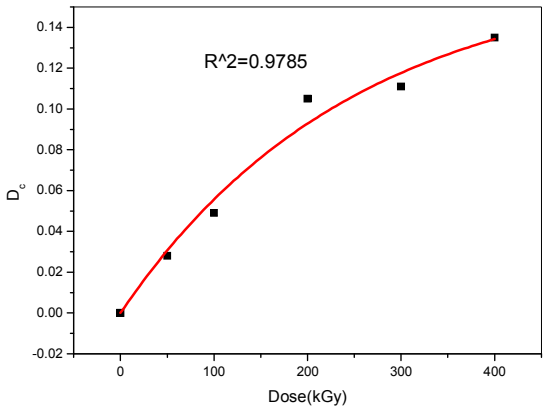

Fig. 8 - The D_c of PAN precursor fibers at different doses

According to our speculation, the D_c of the irradiated PAN fibers increases quickly with increasing irradiation doses at initial stage and will gradually reach a saturation of 16.75% at unlimited irradiation dose. We think this is reasonable because the limitation of molecules movement leads to inhibiting completely cyclizing during γ-ray irradiation.

Based on the understanding of cyclization mechanism and irradiation inducing structure, we try to give some comprehension for the DSC results, as shown in Fig. 9. First of all, the cyclization mechanism of the molecules without irradiation during heat treatment is shown in Fig. 9 (1). The first N-H bond on amide group in AM breaks away at a lower active energy and makes a nucleophilic attack on the carbon atom of adjacent nitrile groups and then induces cyclization propagation and generates the first exothermal peak 26. We name this cyclization pathway as C 1. Then another N-H bond on amide group is attracted by the carbonyl group to form hydroxy and the O-H bond will break at a higher active energy and then induce cyclization propagation and generate the second exothermal peak (C 2). As analyzed

above, not only the free radicals but also intermolecular crosslinking took place during irradiation. When a free radical exists in the neighbor position of the amide group before the first N-H bond breaks away, it can reduce the active energy of N-H bond and make the first exothermal peak appear in advance. However, when a crosslinkage exists in the neighbor position of the amide group just before the second N-H breaks away, it can enhance the active energy and make the second exothermal peak appear later. However, the intensity of the second exothermal peak decreases gradually with increasing irradiation doses, which could be ascribed to the partial cyclization induced by irradiation reducing heat release [9,38]. Therefore, the intramolecular cyclization of PAN molecule chain is obtained as shown in Fig. 10.

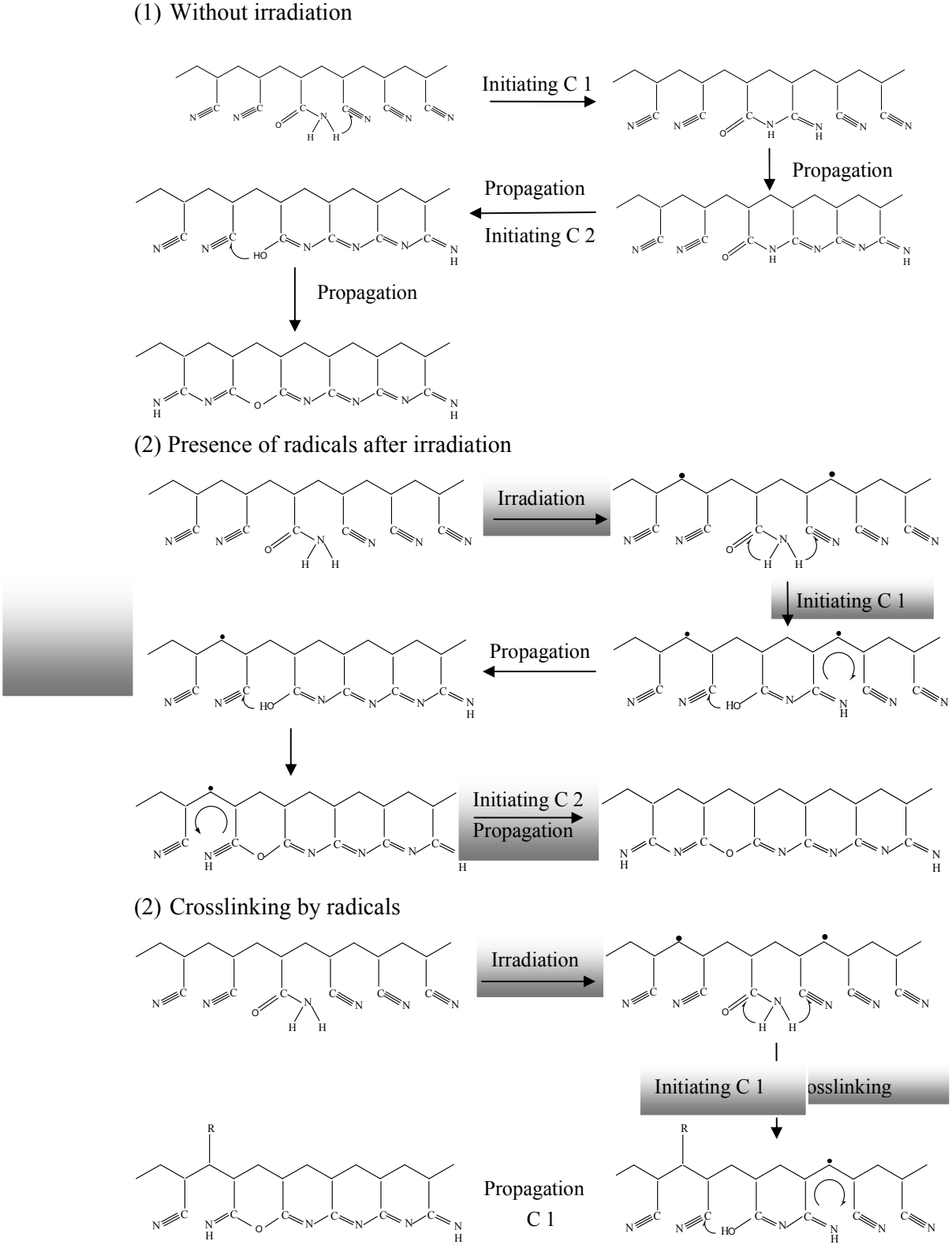

Fig. 9 - Proposed mechanism of cyclization of PAN fibers induced by γ-ray irradiation

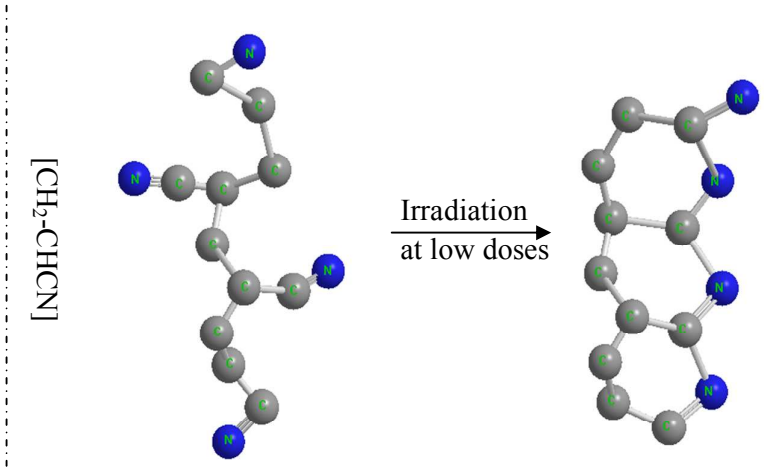

Fig. 10 - A model of intramolecular cyclization of a fragment of a PAN molecule chain –[CH2-CHCN]- at low irradiation doses(< 200 kGy)

3.3 The effect of γ-ray irradiation on the crystalline structure of the PAN fibers

Recently, whether the reactions induced by irradiation only take place in amorphous regions or expand to the crystalline regions is not clear and worthy of our high attention. XRD patterns of the unirradiated and irradiated fibers are shown in Fig. 11 (a). It is noted that the crystalline can be recognized by the sharp diffraction peak at approximately $2\theta = 17^{\circ}$ assigned to the (100) crystallite plane and the weak diffraction peak at approximately $2\theta = 29^{\circ}$ assigned to the (101) crystallite plane [39]. After γ-ray irradiation, the position of both peaks don't change, indicating the remained crystallite structure. However, the intensities of both diffraction peaks unexpectedly decrease with increasing irradiation doses up to 300 kGy. To analyze the microstructure of the crystalline in detail, preferred orientation R, crystallinity X_c and crystallite dimensions (the thickness L_a and width L_c) are listed in Table 1. As we can see, the crystallinity remains almost unchanged at 200 kGy and below,

then gradually decreases from 56.43% at 200 kGy to 52.03% at 400 kGy. It implies that the influence of irradiation on PAN molecules mainly takes place in amorphous regions at lower doses as reported by Liu [9] and the crystallite regions begin to be damaged when the dose increases up to 300 kGy. However, as shown in Fig 11 (b), irradiation has a very slight effect on the preferred orientation of crystallite. With increasing irradiation doses, the values of L_c and L_a for unirradiated to 400 kGy irradiated fibers increases from 11.3 to 13.2 nm and from 23.2 to 27.0 nm respectively, which means that the smaller crystallites located at the edge of the crystallite regions are firstly collapsed by γ-ray irradiation.

Fig. 12 shows that the XRD diffraction patterns of the insoluble in sulfur acid derived from the irradiated fibers at the doses of 200, 300, 400 kGy. It is noted that the sharp peak for crystallite disappears and a new broad diffraction peak appears approximately at $2\theta = 19.4^{\circ}$. Clearly, the crystallite structure changes due to the dissolution by sulfur acid and thus the insoluble is primarily the residue of the amorphous region and a few cyclized and crosslinked molecules. Based on the above results, it is obvious that cyclization and crosslinking induced by γ-ray irradiation mainly occur in amorphous regions.

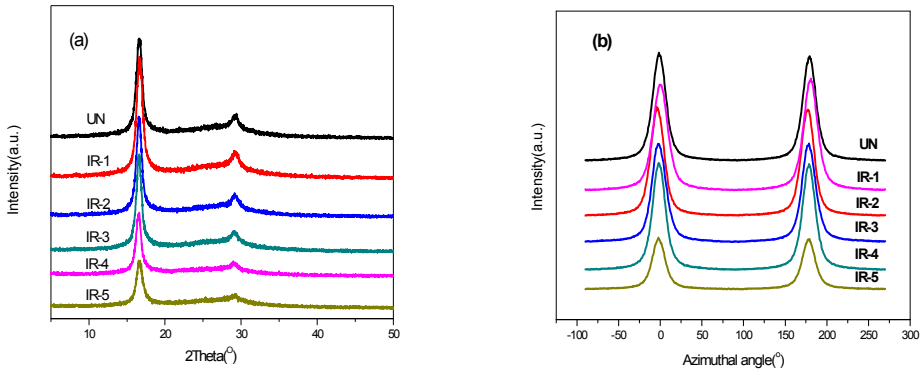

Fig. 11 - XRD patterns of PAN fibers at various doses (a) Equatorial scan; (b) Azimuthal scan on (100) crystal face.

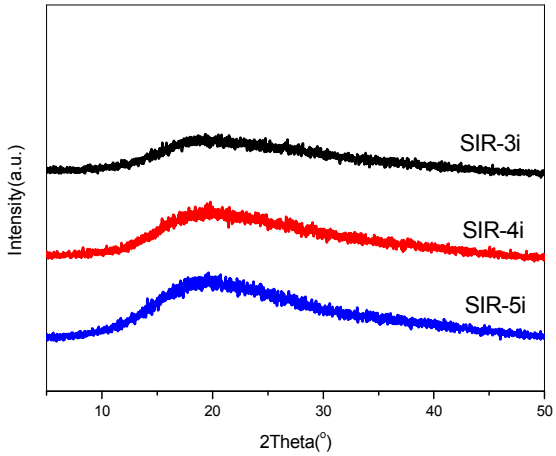

Fig. 12 - XRD patterns of insoluble in sulfur acid derived from 200, 300, 400 kGy.

Table 1 - Crystallite parameters of PAN fibers of different doses .

Dose (kGy)	2*theta* (°)	L_c (nm)	L_a (nm)	X_c (%)	R (%)
0	16.54	11.3	23.2	56.7%	89.5%
50	16.62	12.1	24.6	57.9%	89.3%
100	16.54	12.6	25.7	56.4%	89.6%
200	16.66	12.7	25.9	56.4%	89.4%
300	16.54	13.0	26.5	55.7%	89.1%
400	16.64	13.2	27.0	52.0%	89.6%

3.4 The effect of γ-ray irradiation on the thermal property of PAN fibers during stabilization

In order to convert into carbon fibers, the irradiated PAN fiber with partially cyclized and crosslinked structure still need thermal stabilization, and thermal mechanical analysis can give some guidance on following thermal stabilization [40]. Fig. 13 (a) and (b) shows the strain at a constant initial stress of 12.75 MPa and stress at an initial strain of 0.05% curves of the PAN fibers irradiated at various doses heated by DMA in nitrogen, respectively. As is shown in Fig. 13 (a), there is no obvious difference in strain and all the fibers shrink by about 2% to 175 °C, while there appear stress peaks between 160 - 166 °C due to physical shrinkage in Fig. 13 (b), and the values of stress peak decrease with irradiation doses increasing. Above this temperature, the unirradiated and 50 kGy irradiated fibers extend a little at about 230 °C and then shrink, while the irradiated fibers at the doses beyond 50 kGy shrink greatly above 230 °C. Correspondingly, from 166 to about 230 °C, the stresses for the

unirradiated and 50 - 200 kGy irradiated fibers decay while the stresses for others increase. The higher dose is, the smaller stress decays or the faster it increases. At the range of 273 - 280 ^{o}C, all the fibers shrink to the maximum and begin to extend till break, and the maximum the fibers shrink to increases with further irradiation up to 300 kGy. However, above 300 kGy, the maximum shrinkage of fibers is decreased, i.e, the maximum shrinkage for 300 kGy irradiated fibers is larger than that for 400 kGy irradiated fibers. Correspondingly, the stress increases to the maximum and then begins to decay, and also up to 300 kGy, the maximum of the stress increases with irradiation increasing and decreases at 400 kGy.

According to our knowledge, the strain and stress behaviors are determined by two actions above 175 ^{o}C, one is the sliding between molecule chains due to nitrile groups force decays and the other is the shrinkage due to cyclization of nitrile groups [41]. The existence of crystallites as well as at 175 - 230 ^{o}C and the crosslinked structure induced by irradiation prevent the sliding between the molecule chains at higher temperature. Therefore, up to 300 kGy, the higher dose is, the more the fibers shrink or the higher the stress arrives because irradiation of higher doses generates more crosslinking inhibiting the sliding greatly. When the irradiation dose increases to 400 kGy, the damage of crystallite and generation of more cyclized structure during irradiation make the molecules chains slide easily and lead to less shrinkage than that of 300 kGy. After 335 ^{o}C, the crosslinking is overcome, resulting in the fibers extension or stress decay till break.

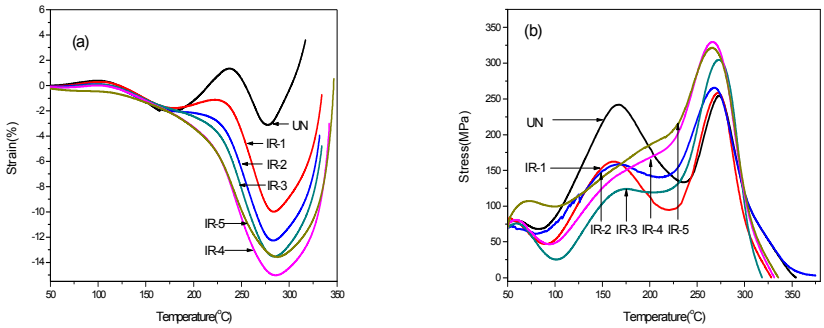

Fig. 13 - The thermal (a) strain and (b) stress curves of PAN fibers irradiated at various doses during stabilization in nitrogen. Negative values represent fiber shrinkage and positive values represent fiber elongation.

The final strains of the PAN fibers during stabilization in air at a series of constant stress are further investigated, as shown in Fig. 14. Based on our previous results, applying appropriate stress on fibers is necessary to restrict the disorientation during thermal treatment [5,7]. From Fig. 14，as the applied stresses increases, the shrinkage for all the final stabilized fibers is decreased gradually or the extension is increased. On the contrary, at the same initial stress, the shrinkage is increased or the extension is decreased with increasing irradiation doses. It is notable that other fibers break at 27 MPa, but only the 400 kGy irradiated fibers don't and extend by 18.81%. This suggests that the PAN molecule chains are cured through crosslinking induced by γ-ray irradiation, which is benefit for amplifying manipulation range of applied stress during stabilization process. Thus we expect to maintain the orientation of PAN molecule chains and obtain high performance carbon fibers through irradiation technology.

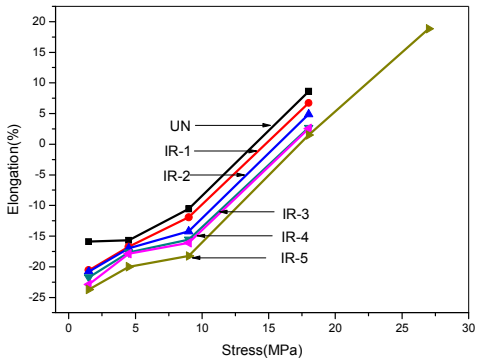

Fig. 14 - The elongation curves of PAN fibers irradiated at various doses during stabilization at a series of constant stress: 1.5, 4.5, 9, 18 and 27 MPa. Negative values represent fiber shrinkage and positive values represent fiber elongation.

4. Conclusions

γ-ray irradiation not only induced cyclization but also intermolecular crosslinking in PAN fibers, and PAN molecular structure mainly took place in amorphous regions at lower doses and then extended to crystalline regions at higher doses than 300 kGy. During the irradiation, the crystallite orientation was well maintained.

Additionally, the exothermic behavior of cyclization reaction was significantly alleviated and the sliding of molecules was prevented by the crosslinking introduced by γ-ray irradiation during stabilization, which might effectively inhibit the thermal disorientation of PAN fibers during the following stabilization and alleviate the skin-core structure due to the lack of oxidation in the fiber core.

Acknowledgements：

Financial support of this work by the National Natural Science Foundation of China (No.51372037) and the National Basic Research Program of China ('973 Program', No. 2011CB605603) is gratefully acknowledged

Notes and references:

1 M.S.A. Rahaman, A.F. Ismail, A. Mustafa, *Polym. Degrad. Stab*., 2007, 92, 1421-1432.

2 Z. Bashir, *Carbon,* 1991, 29, 1081-1090.

3 J. Liu, P.H. Wang, R.Y. Li, *J. Appl. Polym. Sci*.,1994, 52, 945-950.

4 E. Fitzer, W. Frohs, M. Heine, *Carbon*, 1986, 24, 387-395.

5 X.Y. Qin, Y.G. Lu, H. Xiao, Y.C. Hao, D. Pan, *Carbon*, 2011, 49, 4598-4600.

6 D.D. Edie, *Carbon*, 1998, 36, 345-362.

7 X.Y. Qin, Y.G. Lu, H. Xiao, W.Z. Zhao, *Polym. Eng. Sci.,* 2013, 53, 827-832.

8 B.M. Tarakanov. *Fiber Chem*, 1996, 27, 150-154.

9 W.H. Liu, M.H. Wang, Z. Xing, Y.N. Qi, G.Z Wu, *Radiat. Phys. Chem.,* 2012, 81, 622-627.

10 S.M. Pawde, K. Deshmukh, *J. Appl. Polym. Sci*., 2008, 110, 2569-2578.

11 N. Salah, S.S. Habib, Z.H. Khan, S. Al-Hamedi, F. Djouider, *Radiat. Phys. Chem.,* 2009, 78, 910-913.

12 M. Park, Y. Choi, S.Y. Lee, H.Y. Kim, S.J. Park, *J. Ind. Eng. Chem.,* 2014, 20, 1875-1878.

13 H.W. Yuan, Y.S. Wang, P.B. Liu, H.W. Yu, B. Ge, Y.J. Mei, *J. Appl. Polym. Sci*., 2011, 122, 90-96.

14 P.K. Miao, D.M. Wu, K. Zeng, G.L. Xu, C.E. Zhao, G.Yang, *Polym. Degrad. Stab*., 2010, 95, 1665-1671.

15 A.K. Naskar, R.A. Walker, S. Proulx, D.D. Edie, A.A. Ogale, *Carbon,* 2005, 43,1065-1072.

16 M.C. Paiva, P. Kotasthane, D.D. Edie, A.A. Ogale, *Carbon*, 2003, 41, 1399-1409.

17 M.R. Murthy, S. Radhakrishna, *Pramana*, 1983, 20, 85-90.

18 R. Sonnier, A.S. Caro-Bretelle, L. Dumazert, M. Longerey, B. Otazaghine, *Radiat. Phys. Chem.,* 2015, 106, 278-288.

19 S. Ghosal, M. Mukhopadhyay, R. Ray, S. Tarafdar, *Physica A.,* 2014, 400, 139-150.

20 Y.A. Aggour, M.S. Aziz, *Polym. Test.,* 2000, 19, 261-267.

21 W.H. Liu, M.H. Wang, Z. Xing, G.Z. Wu, *Radiat. Phys. Chem.,* 2012, 81, 835-839.

22 W.W. Zhao, Y. Yamamoto, S. Tagawa, *Chem. Mater.,* 2009, 11, 1030-1034.

23 S.M. Badawy, A.M. Dessouki, *J. Phys. Chem. B.,* 2003, 107, 11273-11279.

24 Q. OuYang, L. Cheng, H.J. Wang, K.X. Li, *J. Therm. Anal. Calori.,* 2008, 94, 85-88.

25 S. Arbab, H. Mirbaha, A. Zeinolebadi, P. Nourpanah, *J. Appl. Polym. Sci*., 2014,131, DOI: 10.1002/APP.40343.

26 A.Q. Ju, S.Y. Guang, H.Y. Xu, *Carbon*, 2013, 54, 323-335.

27 X.Y Qin, Y.G Lu, H. Xiao, Y. Wen, T. Yu, *Carbon*, 2012, 50, 4459-4469.

28 A.A. Ogale, C Lin, D.P. Anderson, K.M. Kearn, *Carbon*, 2002, 40,1309-1319.

29 N.U. Nauyen-Thai, S. C. Hong, *Macromolecules*, 2013, 46, 5882-5889.

30 K.I. Lee, J. Li, B. Fei, J.H. Xin, *Polym. Degrad. Stab*., 2014, 105, 80-85.

31 J. Mittal, O.P. Bahl, R.B. Mathur, N.K. Sandle, *Carbon*, 1994, 32, 1133-1136.

32 K.M. Jain, M. Balasubramanian, P. Desai, A.S. Abhiraman, *J. Mater. Sci.,* 1987, 22, 301-312.

33 C. Rottmair, A. Volek, A. Jung, P.C. Chau, B. Fathollahi, *Carbon*, 2007, 45, 3052-3055.

34 D.J.T. Hill, A.P. Lang, J.H. Odonnell, P.J. Pomery, *Polym. Degrad. Stab*., 1992, 38, 193–203.

35 N. Xu, W.N. Fu, L.F. Cao, X.H. Liu, J.L. Zhao, H. Pan, *Plasma Chem. Plasma Process.,* 2014, 34, 1387-1402.

36 W.X. Zhang, J. Liu, G. Wu, *Carbon,* 2003, 41, 2805-2812.

37 H. Xiao, Y.G. Lu, M.H. Wang, X.Y. Qin, W.Z. Zhao, J. Luan, *Carbon*, 2013, 52, 427-439.

38 L. Tan, A.J. Wan, *Mater. Lett.,* 2011, 65, 3109-3111.

39 M.J. Yu, Y.J. Bai, C.G. Wang, Y. Xu, P.Z. Guo, *Mater. Lett.,* 2007, 61, 2292–2294.

40 J. Simitzis, S. Soulis, *Polym. Int.,* 2008, 57, 99-105.

41 A. Gupta, I.R. Harrison, *Carbon*, 1996, 34, 1427-1445.